HYBRID COMPOSITES FOR LH2 FUEL TANK STRUCTURE

Brian W. Grimsley, Roberto J. Cano, and Norman J. Johnston
NASA Langley Research Center, Hampton, Virginia 23681

Alfred C. Loos
Virginia Polytechnic Institute and State University, Blacksburg, Virginia 24061

William M. McMahon
NASA Marshall Space Flight Center, Huntsville, Alabama 35812

ABSTRACT

The application of lightweight carbon fiber reinforced plastics (CFRP) as structure for cryogenic fuel tanks is critical to the success of the next generation of Reusable Launch Vehicles (RLV). The recent failure of the X-33 composite fuel tank occurred in part due to microcracking of the polymer matrix, which allowed cryogen to permeate through the inner skin to the honeycomb core. As part of an approach to solve these problems, NASA Langley Research Center (LaRC) and Marshall Space Flight Center (MSFC) are working to develop and investigate polymer films that will act as a barrier to the permeation of LH2 through the composite laminate. In this study two commercially available films and eleven novel LaRC films were tested in an existing cryogenics laboratory at MSFC to determine the permeance of argon at room temperature. Several of these films were introduced as a layer in the composite to form an interleaved, or hybrid, composite to determine the effects on permeability. In addition, the effects of the interleaved layer thickness, number, and location on the mechanical properties of the composite laminate were investigated. In this initial screening process, several of the films were found to exhibit lower permeability to argon than the composite panels tested.

KEY WORDS: Permeability, Film, Interleaf

1.0 INTRODUCTION

The next generation of reusable launch vehicles (RLV) will require new and innovative materials to meet the goal of cutting the cost of launching payloads into orbit from the current $10,000 per pound to $1,000. One of the most critical issues in the design of this new vehicle is the development of durable, lightweight, cryogenic propellant tanks. The cryogenic tanks are the dominating components of the vehicle structure [1]. Thus, the application of lightweight carbon

fiber reinforced plastics (CFRP) to these components is one of the most promising but challenging technologies for achieving the drastic reduction of empty/non-payload and structural weight.

The sandwich CFRP LH2 tank of the X-33 Demonstrator was ground-tested at Marshall Space Flight Center on November 3, 1999. The tank failed this validation test when the outer skin and core of the sandwich separated from the inner skin, in part due to microcracking of the polymer matrix in the composite inner skin [2]. When the polymer experiences the extremely low temperatures associated with the cryogenic propellant, the material shrinks. The polymer matrix has a higher coefficient of thermal expansion (CTE) than the carbon fiber reinforcement and, therefore, will shrink or strain more upon cooling. The fiber with a near zero CTE acts to resist this strain and internal stresses build up in the matrix. If the stress is sufficiently high, it causes microscopic cracks to form within the composite. The microcracking in the matrix creates a sort of maze for the pressurized LH2 to traverse and enter the honeycomb core. The failure occurred after the tank had been emptied and had heated to -73°C. At this temperature, the microcracks close due to expansion of the polymer matrix. Then, the gas created by evaporation of the LH2, having no free volume to expand, built up pressure in the core causing the inner composite skin to rupture. This failure of the CFRP LH2 tanks represented a major setback for the X-33 program.

The Advanced Materials and Processing Branch at NASA Langley Research Center (NASA LaRC) is working in cooperation with Marshall Space Flight Center (MSFC) on an approach to solve the problems associated with the failure of the cryogenic propellant tanks. It involves introducing a layer or layers of polymeric film into (interleaving) or onto (coating) the composite inner skin that will act as a barrier and contain the LH2 fuel in the presence of microcracks. Ideal candidate films will have the lowest possible permeability factor to LH2. The permeability factor is a measure of the amount of gas that can penetrate, or permeate, through a barrier in a given time [3]. Both commercially available films and novel LaRC polymeric films are being investigated. These candidate films are listed in Table 1. The research at NASA LaRC has centered on developing these films and placing them into CFRP coupons. Selected interleaf composite coupons are also listed in Table 1. The hybrid composite coupons and related films developed in this study were sent to an existing cryogenics test laboratory (currently at MSFC) where they were evaluated as viable barriers to gaseous argon permeation at room temperature. In addition, a study was performed on the effects of film interleaves on the mechanical properties of unidirectional composite laminates.

2.0 MATERIALS

2.1 Aluminized Mylar™ Mylar™ is the Dupont[1] trade name for poly(ethylene terephthalate) or PET. It is a condensation homopolyester made from dimethyl terephthalate and ethylene glycol, and has the repeat structure $(–O\text{-}CO\text{-}C_6H_6\text{-}CO\text{-}O\text{-}CH_2\text{-}CH_2\text{-})_n$. Mylar™ polyester film retains good physical properties over temperatures ranging from -70°C to 150°C [4]. It is also useful at temperatures ranging from -250°C to 200°C when the physical requirements are not as

[1] The use of trademarks or names of manufacturers in this report is for accurate reporting and does not constitute an official endorsement, either expressed or implied, of such products or manufacturers by NASA.

demanding. Various studies have been conducted on Mylar™ as a candidate material for aerospace use. It has been used on various unmanned missions and on satellites for thermal protection. A study was conducted at NASA Lewis Research Center in the late 1960's to qualify Mylar™ films for use in the Saturn rockets [5]. In this case, it was to be used in a cryogenic positive expulsion bladder (CPEB), where cryogenic fluid contained within a bladder is ejected by means of an externally applied force. The research centered on finding barrier materials that remain flexible at cryogenic temperatures and resist failures caused by folding and wrinkling during expulsion cycling. Films that were 6.4 μm thick were found to remain sufficiently flexible at cryogenic temperatures to perform expulsion although some diffusion of LH2 occurred. Another study from the same period showed that, at temperatures approaching -273°C (0^{o}K), semi-crystalline Mylar™ exhibits the properties shown in Table 2 [6].

Table 1. Barrier candidate films.

Film/Composite	Item Designation	Source	Item Quantity	Item Thickness, mm
Aluminized Mylar™	DE051-A	Dunmore	1	.023
Aluminized Mylar™	DE051-B	Dunmore	1	0.1
Self-Metallizing Silver Film	RES6-54	LaRC	2	0.09-0.11
Vectra A950	G30921	Ticona	2	0.04
Polyimide 2+1	DD329-43	LaRC	1	0.04
Polyimide 2+1	DD329-55	LaRC	1	0.025
Polyimide 2+1	DD329-47	LaRC	1	0.04-0.05
Polyimide 2+1	DD329-48	LaRC	1	0.04-0.05
Polyimide 3+4	DD329-41	LaRC	1	0.055
Phenoxy	TM299	LaRC/API	3	0.05
Phenoxy-clay	TM300	LaRC/API	3	0.05
Polyimide Hybrid	PC351-13-3	LaRC	1	0.91
IM7/977-2 Composite	AU503	LaRC	1	0.91
Composite/Phenoxy Interleaf	AU504	LaRC	1	0.94
Composite/Phenoxy-Clay Interleaf	AU505	LaRC	1	0.94
Composite/(1mil) Al-Mylar Interleaf	AU512-1	LaRC	1	0.94
Composite/(4mil) Al-Mylar Interleaf	AU512-2	LaRC	1	1.04
Composite/Silver PI Film Interleaf	AU512-3	LaRC	1	0.99

In order to improve upon the barrier properties of the Mylar™ film, it was coated with 99.9% pure aluminum by physical vapor deposition at the Dunmore Corporation. The Mylar™ film designated DE051-A has a 300 angstroms thick aluminum coating on both sides while the film designated DE051-B is coated on one side only.

Table 2. Cryogenic mechanical properties of Mylar™ film.

Toughness	6.0 MPa
Modulus	10.5 GPa
Strength at 5%strain	0.3 GPa

2.2 Self-Metallized Polyimide The two films labeled RES6-54 were prepared at NASA-LaRC in a single-stage metallizing procedure. As opposed to aluminized Mylar™, where the metal surface is deposited onto a polymer film or substrate. In this procedure, the metallized film is developed from a single solution containing both the native metal and the poly(amic acid) of the

final polyimide [7]. For these films, a silver (I) ion-doped BTDA/4,4'-ODA solution was cast onto a glass substrate. The cast solution was then thermally treated to induce an internal metal ion reduction. These silver (0) atoms then aggregrate to the film surface while the amic acid undergoes imidization. The thin surface layer (5 to 9.9% Ag) was found to have an outstanding metal-polymer adhesion and exhibits excellent specular and surface conductivity while maintaining the mechanical characteristics of the parent polyimide [7].

2.3 Vectra™ Film Vectra™ A950 is a liquid crystal polymer (LCP), one of a family of aromatic copolyesters produced by Hoechst Celanese Corporation, now Ticona Polymers. LCPs were first discovered in the 1950's and offer excellent high-temperature thermal-stability, and high rigidity and strength at cryogenic temperatures. LCPs have rigid, rod-like microstructures that, when melted, align into highly ordered configurations. Sperling [8] uses the analogy of a kitchen sink filled with floating toothpicks (rod-like phase) and water (random coil phase) to describe LCPs. At first, as the material becomes molten, the toothpicks are random in order. However, as the surface becomes more concentrated, the toothpicks begin to align into small groups more or less side by side, creating two phases, the dilute disordered phase and the liquid crystal phase. The toothpicks order themselves to prevent one toothpick from having to go through or over another. This allows fabrication of finished neat resin parts that are anisotropic, that is, having a higher strength and stiffness in the direction that the rods have aligned. The alignment of these rods also allows for zero shrinkage of parts along this axis of orientation which translates into parts with exceptional tolerances [9]. Some physical and mechanical properties of Vectra™ A950 provided by *Ticona Polymer* are presented in Table 3.

Table 3. Properties of Vectra™ A950 film at room temperature.

Density	1.40g/cc
CTE	$10x10^{-6}/^{o}C$
Melting Point	340°C
Tensile Strength	0.17 GPa
Tensile Modulus	15.5 GPa
Elongation at Fracture	1.5%
Flexural Strength	0.15 GPa
Flexural Modulus	9.7 GPa
Charpy Impact Strength	0.11 J/m^2

In addition to these properties, Vectra™ retains 70% of its impact value down to about -270°C.

2.4 Inorganic-Organic Films New organic-inorganic nanocomposites, also called inorganic-organic polymers, are being developed at NASA LaRC for potential use as films, adhesives and matrix materials for carbon-fiber-reinforced-composites. These materials have the potential to enhance the barrier properties of LH2 propellant tanks due to their nanosize and high aspect ratios. The organo-clay platelets can have aspect ratios from 20 to 2000 and plate spacing can be on the order of 36 angstroms [10]. In addition to enhanced barrier properties, the nanoclays are lightweight and can therefore increase specific strength, which is crucial in aerospace design.

2.4.1 Polyimide/Nano-Clay Films The basic approach to synthesize organo-clays is to first modify the inorganic material (clays) [11]. This involves exfoliation of all the inorganic cationic material (Na^{+}, Ca^{++}, etc) that occupies the spacing between the clay plates using organic quaternary salts. Once exfoliated, the spacing is filled with small organic molecules that are compatible with polymers and the organoclay can be dissolved or blended into the polymer. The nanoclay-modified polymer can be cast into films or combined with carbon fiber to form prepreg. Five films were cast and thoroughly imidized using various formulations of SCPX-2003 organoclay in polyimide acid (BTDA-3,3'ODA) solutions. Also, a Cloisite 30B organoclay was combined with a linear thermoplastic epoxy (Phenoxy) resin obtained from Applied Polyamic, Inc. These formulations are detailed in Table 4.

Table 4. LaRC™ nano-clay films.

Film Designation	Polymer	Clay	Volume % Clay
DD329-43	BTDA-3,3'ODA	None	N/A
DD329-55	BTDA-3,3'ODA	SCPX-2003	0.82
DD329-47	BTDA-3,3'ODA	SCPX-2003	2.97
DD329-48	BTDA-3,3'ODA	SCPX-2003	4.92
DD329-41	BTDA-3,3'ODA	SCPX-2003	2.78
TM299	Phenoxy	None	N/A
TM300	Phenoxy	Cloisite 30B	5.00

2.4.2 Phenylethynyl-Containing Imide Silanes The film designated PC 351-13-3 in Table 1 is composed of an oligomeric organic precursor containing phenylethynyl and silane groups, and an inorganic precursor. A pendant phenylethynyl imide oligomeric disilane (PPEIDS) and tetraethoxysilane (TEOS) are used to formulate a sol-gel solution in N-methyl-2-pyrrolidinone (NMP). Distilled water is added to the stirred solution to hydrolyze the trialkoxy silane groups at the chain ends of the PPEIDS organic precursor. The TEOS then bonds to the chain at these sites to form a silica-containing hybrid structure. The sol-gel is then cast on a glass plate, dried, and cured at 371°C. The film is reported to have an elastic modulus of 3.7 (+/-0.4) GPa and tensile strength of 110(+/-17.2) MPa at ambient temperature [12].

2.5 Composite Materials The composite used in the face-sheets of the LH2 propellant tank was Cycom™ IM-7/977-3. The prepreg is supplied by Cytec-Fiberite. The manufacturer supplied properties of 977-3 toughened epoxy base resin and IM-7/977-3 composite are shown in Table 5.

Table 5. Mechanical properties.

977-3 Neat Resin	Tg	232°C
	Density	1.28 g/cc
	Tensile Strength	6.9 MPa
	Tensile Modulus	3.6 GPa
	Flexural Strength	137.8 MPa
	Flexural Modulus	3.7 GPa
IM7/977-3 Composite	0° Tensile Strength	1.8 GPa
	0° Tensile Modulus	152 GPa
	Failure Strain	1.3%
	Poisson's Ratio	0.35
	0° Compressive Strength	1.6 GPa
	0° Compressive Modulus	124 GPa
	Interlaminar Shear Strength	0.14 GPa

The unidirectional prepreg material was cut and hand-placed on a flat caul plate and vacuum bagged. The bagged prepreg laminate was autoclave cured utilizing the following cure cycle. The material was heated from 20°C to 120°C at 1°C/min and held at 120°C for 60 min to devolitalize the solvents. At 30 minutes into this first temperature hold, the autoclave was pressurized to 0.7 MPa. The temperature of the part was then increased at 1°C/min to the final cure temperature of 177°C and held at 177°C for 120 min. The part remained under full vacuum throughout the process.

Six eight-ply quasi-isotropic lay-up $[0/90/45/-45]_s$ panels were fabricated and submitted for barrier property characterization (Table 1.0). A control panel, AU503, was fabricated without the film interleaf. Panels designated AU504, AU505 and AU512-1 through 3 were fabricated using the same ply stacking sequence and processing cycle as the control, but with a layer of film placed at the center of the lay-up. The films were of the same type described in Table 1. The ply stacking sequence is represented as follows: [0/90/45/-45/film/-45/45/90/0]. Panel AU504 contained a 2 mil thick phenoxy film, AU505 contained a nano-clay/phenoxy film, AU512-1 contained a 1mil thick double-sided aluminized Mylar™, AU512-2 contained a 4 mil thick single-sided aluminized Mylar™ interleaf, and AU512-3 contained a self-metallizing silver/polyimide film interleaf. The panels fabricated with the interleaf film layer were examined using the pulse-echo C-Scan technique and determined to be of good quality.

In addition, twelve unidirectional composite panels were fabricated for mechanical testing using the IM7/977-3 epoxy prepreg and aluminized Mylar films of 0.25, 1, and 4 mil thicknesses. These panels were processed in a vacuum hot press using the cure schedule described above. The resulting panels were C-scanned and sections were photo-micrographed to evaluate consolidation quality and void content.

3.0 PERMEABILITY TESTING

Permeability characterization of the films and interleaf composites was performed at MSFC cryogenics laboratory in accordance with ASTM D-1434, "Standard Test Method for Determining Gas Permeability Characteristics of Plastic Film and Sheeting, Method V – Volumetric." For the purpose of this initial characterization of permeation at room temperature, one film from each category listed in Table 1 was tested one to six times and the averages reported in Table 6. For convenience, argon with a molecular diameter of 2.94 E-8 cm was used as a penetrant gas in place of hydrogen with a molecular diameter of 2.34 E-8 cm calculated from Van der Waal's equation.

3.1 Permeability Test Methodology In the test method, a sample is mounted horizontally between two chambers in the volumetric gas transmission cell. The lower chamber contains the test gas at a specified elevated pressure. The upper chamber is maintained close to atmospheric pressure and receives the permeating gas. The flow of gas through the test specimen is determined by measuring the displacement of a slug of liquid in a capillary tube. From the measurements of the capillary slug position versus elapsed time, the volume flow rate and gas transmission rate can be calculated. The permeance was calculated as follows:

$$P = \frac{10^{-6} \bullet P_2 \bullet V_r}{A \bullet R \bullet T \bullet (P_1 - P_2)}$$

where, P_1 and P_2 are the pressures in the lower and upper chambers of the cell, respectively, V_r is the volumetric flow rate. A is transmitting area of the specimen, R is the universal gas constant (8.3143×10^3 L·Pa/{mol·K}), and T is the gas temperature. The S.I. units of Permeance are reported here as [mol / (m^2·s·Pa)]. Permeability, P, is determined by incorporating film thickness in the Permeance calculation. Since Permeability requires testing of the same film type at various film thicknesses to ensure material homogeneity, it is not reported here.

3.2 Permeability Test Results The measured leak rate and average permeance for the films and interleaf composites are tabulated in Table 6. Also reported are the Darcy constants and log Darcy constants for each specimen. The Darcy Constant, κ, measured in Darcy units, represents the permeability of a porous medium to viscous flow for the flow of 1cc/s/cm^2 of surface of a liquid of 1 centipoise (cP) viscosity under a pressure gradient of 1atm/cm. The constant provides a useful comparison of the sample properties with any other sample tested [13]. The Darcy constant is independent of the gas properties, temperature, and thickness. It is reported here for the purpose of comparison despite the film homogeneity concerns stated above.

Of the films tested, the phenylethynyl-containing imide silane, or Polyimide Hybrid (PC351-13-3), appears to be the most promising non-metallized barrier as evidenced by its relatively low leak rate, permeance and Darcy constant. The lowest overall permeability was found in the Mylar™ sample having aluminum on both sides (DE051-A). The Mylar™ containing aluminum on one side showed resistance to argon transport in much the same degree as the self metallized silver films. Of the polyimide films containing nanoclays, the sample containing the highest percentage of clay (DD329-48) was found to have the lowest Darcy constant. However, the

addition of the clay did not greatly enhance the barrier property of the parent polyimide nor was any trend apparent in varying the percentage of clay. The phenoxy films did not fare well in comparison to all other films tested and the addition of clay was found to reduce the barrier property in this case.

Table 6. Permeability test results of argon at room temperature.

Film/Composite	Item Designation	Measured Leak Rate (cc/s)	Average Permeance, P (mol/m^2*s*Pa)	Average Darcy Constant, K	Log Average Darcy Constant,
Aluminized Mylar (1mil)	DE051-A	1.78 E-08	5.259E-22	3.74 E-23	-22.43
Aluminized Mylar(4mil)	DE051-B	1.46 E-04	7.516E-18	3.00 E-18	-17.52
Self-Metal Silver (4.5 mil)	RES6-54-A	1.54 E-04	4.693E-18	1.35 E-18	-17.87
Self-Metal Silver (3.5 mil)	RES6-54-B	2.33 E-05	1.372E-18	4.70 E-19	-18.33
Vectra A950	G30921	1.72 E-03	5.208E-17	6.52 E-18	-17.19
Polyimide 2+1	DD329-43	6.12 E-05	5.698E-17	1.04 E-17	-16.98
Polyimide 2+1	DD329-55	2.42 E-04	2.722E-16	3.18 E-17	-16.50
Polyimide 2+1	DD329-47	9.74 E-03	2.984E-16	6.84 E-17	-16.17
Polyimide 2+1	DD329-48	3.25 E-04	2.600E-17	4.56 E-18	-17.34
Polyimide 3+4	DD329-41	4.80 E-05	2.631E-18	2.01 E-17	-16.70
Phenoxy	TM299	3.87 E-02	1.513E-13	4.69 E-14	-13.33
Phenoxy-clay	TM300	3.93 E-01	7.955E-12	2.08 E-12	-11.68
Polyimide Hybrid	PC351-13-3	4.13 E-06	1.220E-19	1.72 E-20	-19.76
IM7/977-2 Composite	AU503	1.01 E-05	3.073E-19	7.87 E-19	-18.10
Composite/Phenoxy	AU504	1.01 E-05	3.444E-19	8.82 E-19	-18.05
Composite/Phenoxy-Clay	AU505	8.13 E-06	2.574E-19	6.84 E-19	-18.16
Composite/(1mil) Mylar	AU512-1	2.25 E-05	6.687E-19	1.85 E-18	-17.73
Composite/(4mil) Mylar	AU512-2	8.02 E-06	2.322E-19	6.97 E-19	-18.16
Composite/Silver PI Film	AU512-3	1.04 E-05	3.718E-19	5.64 E-19	-18.25

The IM7/977-3 composite control panel (AU-503) was found to have a lower permeance and Darcy number for permeation of argon at room temperature than several of the films tested. Of the interleaf panels tested, the 4-mil Mylar™ and the phenoxy with clay were found to show slight improvement over the barrier property of the control panel. The 1 mil aluminized Mylar interleaf panel (AU512-1) exhibited a higher permeability than the control and all other panels tested. This was not as expected due to the fact that DE051-A film had a much lower permeance than any other film tested, especially the phenoxy samples. This would seem to indicate that the (AU512-1) panel was flawed either by higher void-content in the composite or because of some damage inflicted on the film interleaf during handling or processing.

4.0 INTERLEAVED COMPOSITE MECHANICAL TESTING

Test specimens were obtained from the twelve unidirectional composite panels described in Section 2.5 to determine the effects of embedding, or interleaving, the aluminized Mylar film in the composite on the mechanical properties of the composite. These included 20-ply unidirectional specimens for short beam shear (SBS) tests (ASTM D 2344-84) and 10-ply unidirectional specimens for 0^o flexure tests (ASTM D 790-97). The panel stacking sequences as well as the test results are shown in Table 7.

Table 7. Mechanical Properties of Aluminized Mylar™ Interleaved Composites.

Panel Designation	Stacking Sequence	Average Flexural Strength (MPa)	Standard Deviation (MPa)	Average Flexural Modulus (GPa)	Shear Strength 1st Event (MPa)	Shear Strength 2nd Event (MPa)	Standard Deviation 2nd Event (MPa)
051600	$[0]_{10}$ (control)	1981.2	53.1	15.4			
060700	$[0_5$ /1mil/ $0_5]$	1491.9	224.0	14.0			
071000	$[0_5$ /4mil/ $0_5]$	1899.2	138.5	14.0			
071800	$[0_5$ /0.25mil/ $0_5]$	2026.0	211.6	15.8			
072700	$[0_3$ /0.25mil/0_2 /0.25mil/0_2 /0.25mil/$0_3]$	2207.9	103.4	15.6			
051700	$[0]_{20}$ (control)				N/A	114.4	2.1
060800	$[0_{10}$ /1mil/ $0_{10}]$				60.6	109.3	1.0
062900	$[0_{10}$ /4mil/ $0_{10}]$				77.9	105.4	2.5
072100	$[0_{10}$ /0.25mil/ $0_{10}]$				70.3	113.0	2.7
080100	$[0_5$ /0.25mil/0_5 /0.25/0_5 /0.25/$0_5]$				47.6	55.8	2.1

Fracture zones in the SBS specimens show that the aluminum coating had separated from the Mylar™ film during the test. The SBS column labeled "1st event" appears to be failure of the Al-Mylar™ bond. This distinct event was signaled by a small drop in load during the test shown in an example of a measured load/deflection curve Figure 4.1. The SBS test was continued until the load reached a maximum at which point the specimen failed in shear. The flexural and shear strength results are plotted in Figures 4.2 and 4.3.

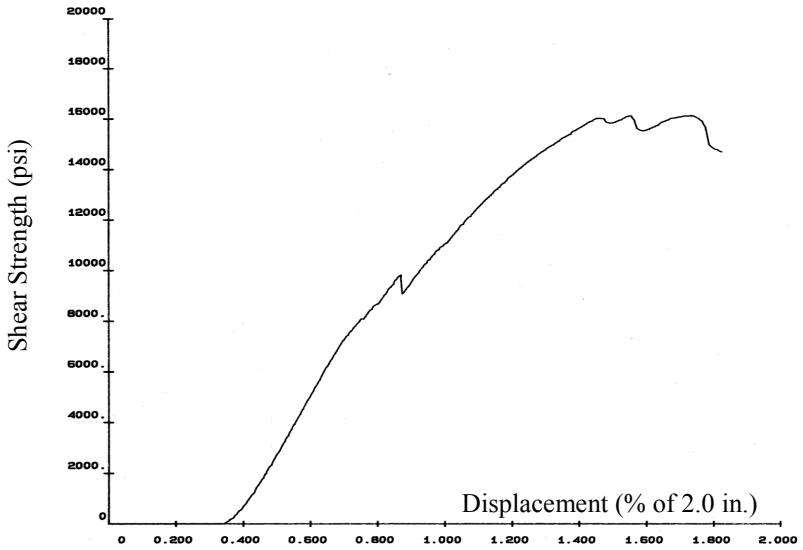

Figure 4.1. Sample load/deflection curve of Al-Mylar™ Interleaf in IM-7/977-3 Composite.

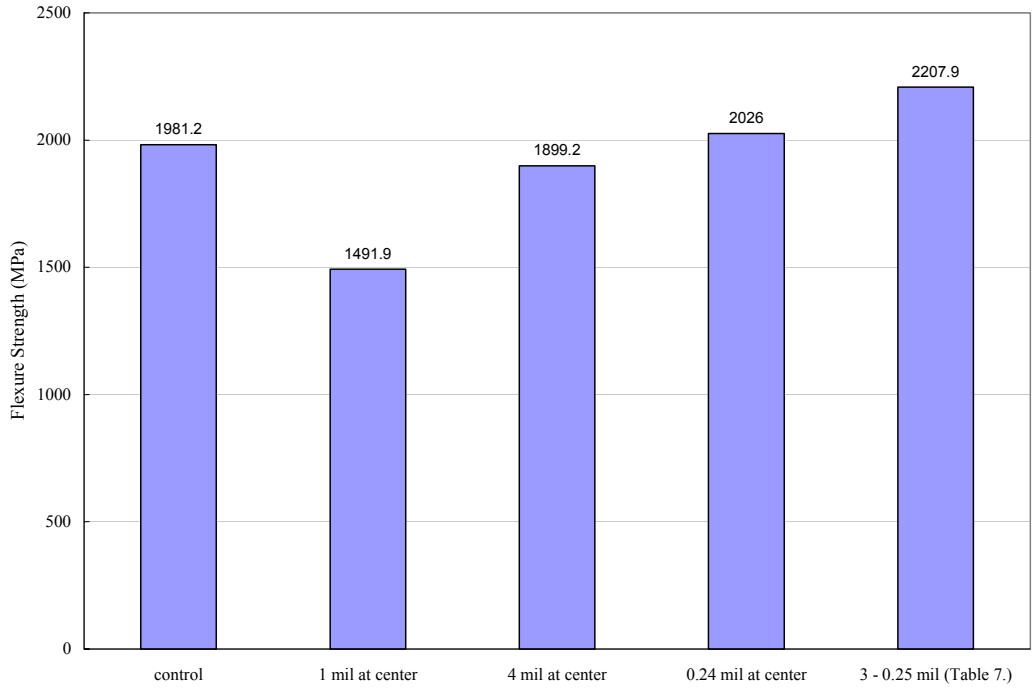

Figure 4.2. Flexural strengths of Al-Mylar^{TM} Interleaf IM-7/977-3 Composites.

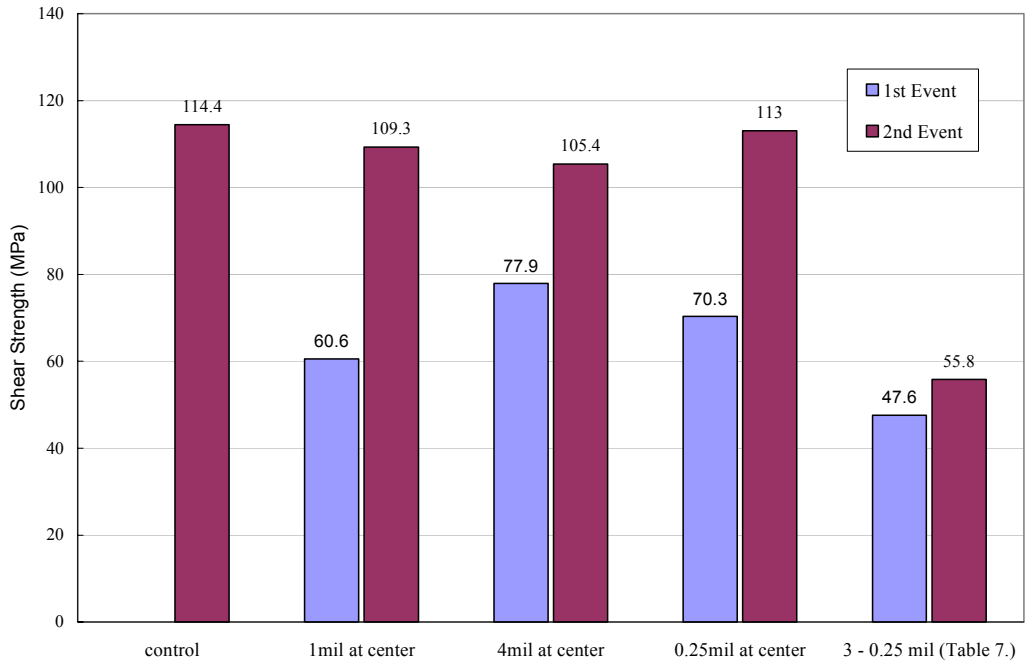

Figure 4.3. SBS data for Al-Mylar^{TM} Interleaf in IM-7/977-3 Composites.

The data for the interleaf coupons show up to a 50% reduction in short beam shear strength and up to a 20% reduction in flexural modulus compared to control panel values. The lowest shear strengths were found in panels fabricated with three plies of 0.25 mil interleaf. Interestingly, this configuration was found to have the highest flexural strength. The flexural strength and modulus were found to increase with decreasing film thickness.

Except for the control panel, which underwent tensile failure, all of the SBS test specimens were found to have failed in shear by complete delamination across the specimen at the aluminum-to-Mylar™ interface rather than at the aluminum-to-epoxy composite interface. The mode of failure for the 0°flex specimens was also delamination at the aluminum-to-Mylar™ bond interface. These results indicate that the aluminum-to-Mylar™ bond is weaker than the aluminum-to-composite bond. However, it is interesting to note that the SBS specimens continued to hold load far past the initial Al-Mylar™ debond and that the final failure strengths, except for the 3-film interleaved specimen, were very close.

5.0 CONCLUSION

Based on the initial results of the permeability tests, the phenylethynyl-containing imide silanes (designated PC 351-18-3) and the aluminized Mylar™ films show the greatest promise as barriers to argon gas at room temperature. Comparing results of the Mylar™ specimens with aluminum coating on one side versus two sides indicates that the barrier properties of aluminized Mylar™ are strongly dependent on the aluminum. Discrepancies found in the reported permeability data for the composite panels versus the films demand further investigation of the effects of processing conditions on the film barrier as well as the permeability test methodology.

Mechanical tests of the interleaved composite panels showed that failure was delamination caused by a weak aluminum to Mylar™ bond. The strength of this bond will have to be improved in order for the Mylar™ to be used as an interleaved barrier material.

6.0 FUTURE WORK

Future work will include fabrication and evaluation of composites containing the PC 351-18-3 interleaved films. Candidate films that exhibit the lowest permeation to argon will be further tested varying film thickness to ascertain the Permeability number. A study will be performed to correlate the permeability data found by the ASTM - Volumetric technique with other techniques found in the literature. The proper stacking sequence of the films within the composite panels will need to be explored to maximize strength and minimize gas permeation while maintaining the low-weight characteristics integral to cryotank success. This will require an in-depth understanding of how gas permeates through both the polymer film and composite. In addition, studies should be conducted varying film thickness and quantity. Mechanical properties of these panels should then be evaluated at ambient and cryogenic temperatures, both before and after thermal cycle preconditioning. Finally, permeation at cryogenic temperatures needs to be evaluated under an applied load to simulate flight conditions.

7.0 ACKNOWLEDGEMENTS

The authors acknowledge the work of the following in developing polymeric films for this study: John W. Connell, Donovan M. Delozier, Paul M. Hergonrother, Cheol Park, Joseph G. Smith, and Robin E. Southward. The authors acknowledge the work of the following in conducting permeability testing at Marshal Space Flight Center for this study: Anthony J. Day and Frank E. Ledbetter.

8.0 REFERENCES

1. Marshall Space Flight Center Homepage, http:www.msfc.nasa.gov/news
2. Final Report of the X-33 Liquid Hydrogen Tank Test Investigation Team, Marshall Space Flight Center, Huntsville, AL, May, 2000.
3. H. Yasuda and V. Stannett, Polymer Handbook, Wiley, 1975, pp. 232-240.
4. Mylar™ Technical Information E.I. DU PONT DE NEMOURS & CO.(INC)
5. R.F. Lark in T.T. Serafini, ed., Cryogenic Properties of Polymers, Marcel Dekker Inc, 1968, pp. 1-16.
6. C.D. Armeniades, I. Kuriyama, J.M. Roe and E. Baer, in ref. 5, pp.155-168.
7. R.E. Southward and Diane M. Stokley, "Reflective and Electrically Conductive Surface Silvered Polyimide Films and Coatings Prepared via Unusual Single-stage Self Metallization Techniques", Progress in Organic Coatings, **41**(1-3),99-119 (2001).
8. L.H. Sperling, Introduction to Physical Polymer Science, Wiley, 1992, pp. 279.
9. A. Kaslusky, "Liquid Crystal Polymers: A Primer", *Advanced Materials and Processes*, December 1993.
10. T. Lan, P.D. Kaviratna, and T. J. Pinnavaia, "Synthesis, Characterization and Mechanical Properties of Epoxy Clay Nanocomposites", *Proceedings of the ACS*, PMSE, 71:527-528.
11. D.M. Delozier, R.A. Orwoll, J.F. Cahoon, N.J. Johnston, J.G. Smith, and J.W. Connell, "Preparation and Characterization of Polyimide/Organoclay Nanocomposites", (in press).
12. C. Park, S.E. Lowther, J.G. Smith, J.W. Connell, P.M. Hergonrother, and T. L. StClair, . "Polyimide-silica hybrids containing novel phenylethynyl imide silanes as coupling agents for surface-treated titanium alloy", *International Journal of Adhesion and Adhesives*, **20**, 457-465 (2000).
13. A.J. Day and C. Upton. "The Room Temperature Helium Permeability of IM7/8553 Graphite Epoxy Material", JANNAF-RTNS Meeting.